Investigation on the Validity of Topology Optimisation Methods

Caroline S. Edwards,* Hyunsun A. Kim† and Chris J. Budd‡
University of Bath, Bath. BA2 7AY, United Kingdom

Evolutionary Structural Optimisation (ESO) is a discrete topology optimisation method. The ESO algorithm slowly removes redundant material aiming to evolve the structure to a fully stressed design. Redundant material is characterised by low von Mises stress, calculated using finite element analysis. Discrete problems are generally considered to be more difficult to solve than continuous problems due to smoothness issues and potential instabilities. A common continuous optimisation approach is to relax the problem then penalise the minimum compliance solution to give a discrete design. A popular such approach is referred to as Solid Isotropic Microstructure with Penalisation (SIMP). We aim to develop a better understanding of both the ESO and SIMP problem formulations and methodologies by investigating a challenging test problem. Initial analysis of the test problem shows that both ESO and SIMP are unable to converge to an intuitive solution. The reason for this failure in both cases relates to an inappropriate objective function of the optimisation methods and also to detailed aspects of the numerical implementation. We therefore suggest a more appropriate objective function for ESO's fully stressed design algorithm. Based on the new objective function we apply ESO to the test problem with a carefully refined mesh. The numerical results indicate that the new objective function finds optima which are indeed close to a fully stressed design.

I. Introduction

Topology optimisation is a method for finding the optimal material distribution within a fixed design domain Ω. An optimum can be defined by various objective functions such as minimum compliance or a Fully Stressed Design (FSD), which is a structure with a constant stress field. The design domain is usually discretised using finite elements with the existence or density of the elements being the design variable.

Solving optimisation problems with discrete design variables are generally considered to be more difficult than with continuous design variables.[1] Thus, a typical method used to solve topology optimisation problems is to relax the layout design variable by introducing intermediate states for an element that are between solid and void. This new layout design variable is analogous to the continuous density of the element. However, this density is somewhat artificial and a design with a continuous density distribution cannot be manufactured. Therefore, the intermediate densities are penalised to give them low stiffness thus producing a near discrete solution. This approach is referred to as Solid Isotropic Microstructure with Penalisation (SIMP).[2–4]

Alternatively, there are methods which embrace the discrete layout design variable. One such method is Evolutionary Structural Optimisation (ESO).[5,6] ESO slowly removes redundant material to evolve the structure to an optimum. Redundant material is characterised by low local sensitivity values, that is von Mises stress, calculated using finite element analysis (FEA). It is said that this approach evolves a structure towards a FSD.[7]

*Ph.D. Student, Department of Mechanical Engineering, Student Member AIAA
†Lecturer, Department of Mechanical Engineering, Member AIAA.
‡Professor of Applied Mathematics, Department of Mathematical Sciences.

Unlike SIMP, ESO is a heuristic method derived from engineering intuition; hence it cannot guarantee convergence. However, the research efforts over the last decade have demonstrated numerically that ESO reliably finds an optimal solution.[5–7] To test this, a problem was introduced in Ref. 8 to investigate the validity of the ESO strategy. When ESO was applied to the problem, it was found that removing the element with the lowest sensitivity value increased the total compliance by a factor of 10. This removal fundamentally changed the way the loads were transmitted and hence the structure evolved to a sub-optimal solution.

Inspired by such an interesting result, the current paper further investigates the test problem of Ref. 8 with the aim of developing a better understanding of the formulations and methodologies for both the ESO and SIMP optimisation problems.

In the following section we briefly outline the optimisation problem formulations for the SIMP and ESO strategies. §III defines the test example used for this investigation. The influence of mesh density is analysed and ESO is applied to a refined mesh in §IV. Similarly, SIMP is applied to the test problem in §V which is followed by the conclusions.

II. Problem formulations for the topology optimisation methods

A. The SIMP optimisation approach and algorithm

The SIMP formulation is based on the continuous structural optimisation problem of minimising the total compliance C of a structure parameterised by a vector of coordinates $\boldsymbol{\xi} \in \Omega$ with constant volume V_c,

$$\left.\begin{array}{rcl} \min & : & C \\ \text{subject to} & : & V \leq V_c \end{array}\right\}. \tag{1}$$

A set of n finite elements over $\boldsymbol{\xi} \in \Omega$ are used to represent a structure and the optimisation problem is constrained to satisfy the elastic equilibrium equation. Hence, the structural displacement, $\mathbf{u}(\boldsymbol{\xi})$, under the given loads is a design variable.

The presence or layout of material, $x(\boldsymbol{\xi})$, within the design domain is also a design variable. This discrete variable is relaxed so that it is continuous over $[0, 1]$. The intermediate values are penalised by applying a factor 'p' (typically $p \sim 3$) to the elemental density to steer the solution to a discrete topology. Thus SIMP is defined as finding the optimal penalised material distribution $x(\boldsymbol{\xi})^p$, $p > 1$, where

$$\int_\Omega x(\boldsymbol{\xi}) d\Omega \leq V_c; \;\; 0 \leq x(\boldsymbol{\xi}) \leq 1, \;\; \boldsymbol{\xi} \in \Omega. \tag{2}$$

When using FEA, $\mathbf{K}_i$ is defined as the element stiffness matrix and $\mathbf{u}_i$ the element displacement vector for an element i. Thus total compliance for $\mathbf{x} = \{x_1, x_2, \ldots, x_n\}$ is defined as

$$C(\mathbf{x}) = \sum_i x_i \mathbf{u}_i \mathbf{K}_i \mathbf{u}_i. \tag{3}$$

The penalisation of SIMP modifies the problem to the minimisation of penalised total compliance, where penalised compliance is defined as[9]

$$C_p(\mathbf{x}) = \sum_i x_i^p \mathbf{u}_i \mathbf{K}_i \mathbf{u}_i. \tag{4}$$

The SIMP optimisation problem is thus defined as

$$\left.\begin{array}{rcl} \min\limits_{\mathbf{x},\mathbf{u}} & : & C_p(\mathbf{x}) = \sum\limits_{i=1}^{n} x_i^p \mathbf{u}_i^T \mathbf{K}_i \mathbf{u}_i \\ \text{subject to} & : & V(\mathbf{x}) \leq V_c \\ & : & \mathbf{K}\mathbf{u} = \mathbf{f} \\ & : & \mathbf{0} < x(\boldsymbol{\xi})_{min} \leq x(\boldsymbol{\xi}) \leq \mathbf{1} \end{array}\right\}, \tag{5}$$

where $\mathbf{K}$ denotes the global stiffness matrix, $\mathbf{f}$ the load vector, which together they form the elastic equilibrium equation, $x(\boldsymbol{\xi})_{min}$ is a vector of minimum densities to avoid singularities and $V(\mathbf{x})$ is the total material volume.

SIMP has a well defined objective function and the optimisation problem in Eq. (5) can be tackled using a variety of sophisticated algorithms such as the MMA algorithm[10] and still retain the same objective function. We implement SIMP optimisation in this paper by adapting the MATLAB[11] code of Ref. 9, which achieves the objective function by a simple local descent method.

B. The ESO approach and algorithm

ESO optimises a structure by removing material with low stress from the design domain and it is said that this leads to a FSD.[5] However, the problem formulation for ESO has not been clearly defined.

ESO also employs FEA to compute the stress field $\boldsymbol{\sigma}$. Hence ESO is subject to the elastic equilibrium equation making $\mathbf{u}(\boldsymbol{\xi})$, the structural displacement, a design variable. ESO has one other design variable x which represents the existence of a finite element. However, unlike SIMP, ESO treats x as a discrete variable and takes a value of either '1' when an element is present or '0' when completely removed.

The removal of elements performed over a number of iterations constantly reduces the volume of a structure. Choosing to remove elements with low von Mises stress, σ_{vm}, has the effect of achieving a more evenly distributed stress field though it can produce locally higher stress at re-entrant corners.

We propose that an objective function of ESO is to minimise the normalised standard deviation of the von Mises stress field subject to the equilibrium constraint. The standard deviation is normalised using the mean von Mises stress $\bar{\sigma}_{vm}$. Thus the ESO problem can be written as

$$\left.\begin{array}{rcl} \min\limits_{\mathbf{x},\mathbf{u}} & : & S(\mathbf{x}) = \left\{ \dfrac{\sum_i \left(\frac{\sigma_{vm_i}}{\bar{\sigma}_{vm}} - 1 \right)^2}{\sum_j x_j} \right\}^{1/2} \\ \text{subject to} & : & \mathbf{K}\mathbf{u} = \mathbf{f} \\ & : & x_i \in \{0,1\}\ i = 1,2,\ldots,n. \end{array}\right\}. \tag{6}$$

An outline of the ESO algorithm can be summarised as follows:

1. FEA computes the displacement field
2. The elements with low von Mises stress are removed
3. Steps 1 to 2 are repeated until all elements are removed
4. Select the solution with the lowest objective function, Eq. (6)

In the later sections we adapt the MATLAB code of Ref. 9 to implement ESO and assess the proposed formulation of ESO numerically.

C. Numerical instabilities and filtering

Topology optimisation can often exhibit chequerboard instability for which the topology contains a chequerboard pattern of active and removed elements or of high and low density elements. It has been established that the appearance of these chequerboard patterns is a numerical phenomenon and does not represent an optimal design.[12,13]

A popular heuristic treatment for preventing chequerboard formations is chequerboard filtering or local smoothing of sensitivities similar to low pass filtering in signal and image processing. This filtering technique works by smoothing local sensitivities after analysis and then these smoothed sensitivities are used to modify and optimise the design.

The filter implemented in this investigation is the Bartlett filter which takes a weighted average of sensitivities within a specified region.[14] This specified region is defined by the parameter r_{min}, the radius taken from the centre of the element i.

$$\hat{S}_i = \frac{1}{x_i \sum_j \hat{H}_j} \sum_j \hat{H}_j x_j S_j, \tag{7}$$

where $\hat{S}_i$ is the filtered sensitivity of element i, S_i is the original sensitivity of element i and $\hat{H}$ is the weighting factor for all enclosed elements j within r_{min} and is determined based on the distance between elements i and j, Eq. (8).

$$\hat{H}_j = r_{min} - dist(i,j). \tag{8}$$

III. Tie beam test problem

The tie beam test problem was presented with the aim of highlighting the possible shortcomings of ESO[8] and is used in this investigation for further examination of the optimisation methods ESO and SIMP.

The test problem is an L-shaped clamped beam with a roller support at the top of the vertical section of the beam which is referred to as the vertical tie, Figure 1. There is a vertical tensile load of intensity $L_y = 1.0$ and a horizontal compressive load of intensity $L_x = 2.0$. The Young's modulus (E) is specified as 1 and the Poisson's ratio (ν) is 0. This test problem is modelled using $n = 100$ four node plane stress elements with unit thickness.[8] This mesh, specified as part of the test problem, is particularly coarse as the width of the vertical tie is only one element.

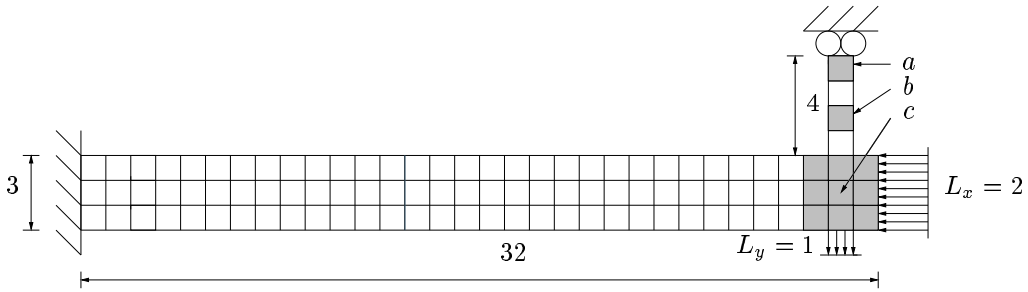

Figure 1. Test problem with a coarse mesh[8] and $V(\mathbf{x}) = 100$

With the objective of optimisation defined as to minimise compliance, the authors of Ref. 8 suggest the design of Figure 2 as an intuitive optimal solution with a total compliance of 1110 and a volume of $V(\mathbf{x}) = 40$. This solution is henceforth referred to as a "tie beam" solution.

In addition to the tie beam solution of Figure 2, there exists a sub-optimal solution which we refer to as a "cantilever" solution in which the roller support at the top is removed and for which the system behaves like a cantilevered beam. An example of a cantilever solution is illustrated in Figure 3.

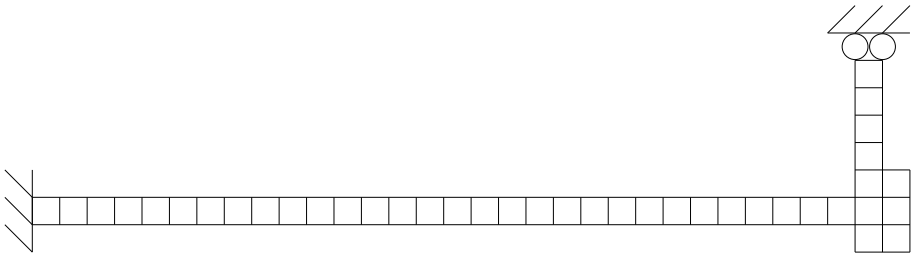

Figure 2. Intuitive optimum with $V(\mathbf{x}) = 40$

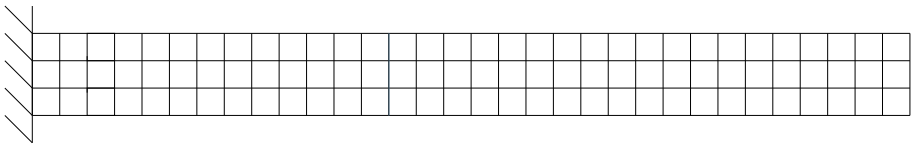

Figure 3. An example of a cantilever solution

In Ref. 8, elemental compliance was used as the sensitivity for ESO as the objective of minimum compliance was considered. When Figure 1 is analysed using FEA, the element with the lowest compliance is identified to be element 'a'. This compliance based ESO algorithm therefore removes element 'a' in the first iteration, which cannot be re-admitted. The removal of element 'a' detaches the beam from the roller support and the beam effectively becomes a cantilever beam, transmitting the vertical load as bending. This change in load transmission increases the total compliance from $C(\mathbf{x}) = 389$ to $C(\mathbf{x}) = 4371$ and leads to a cantilever solution.

When stress based ESO is applied using the von Mises stress as sensitivity instead of elemental compliance, element 'b' of Figure 1 has the lowest von Mises stress and is therefore removed. Once again the total compliance significantly increases to $C(\mathbf{x}) = 4386$ and the total compliance continues to increase monotonically. Hence the structure evolves to a cantilever beam in a similar way to compliance based ESO.

The minimum value of the proposed ESO objective function, $S(\mathbf{x})$, occurs at the initial configuration. After the first iteration, this objective function increases significantly from $S(\mathbf{x}) = 0.099$ to $S(\mathbf{x}) = 0.698$ and does not recover. Therefore, the proposed objective function $S(\mathbf{x})$ is in agreement with the results of Ref. 8, and ESO leads to the sub-optimal cantilever solution.

IV. An application of the ESO approach

In this section, the previously described test problem is analysed and refined. The results of applying ESO to this revised test problem are presented and analysed.

A. Analysis of mesh size and FSD

In order to understand why ESO evolves the topology towards the cantilever beam, we return to its optimisation criterion of FSD. The tie beam configuration primarily transmits the applied loads axially. Thus we simplify the configuration into a pin-jointed truss and ignore the negligible bending stress in region 'c' marked in Figure 1. The simplified system transmits the horizontal load F_x and the vertical load F_y completely to the horizontal beam and the vertical tie respectively.

If we let A_x be the cross-sectional area to which F_x is applied and A_y be the cross-sectional area of the vertical tie which F_y is applied, the approximate von Mises stress is equivalent to the axial stress which in the vertical tie is F_y/A_y, and in the beam is F_x/A_x. Thus for a FSD, we must have

$$\frac{F_x}{A_x} = \frac{F_y}{A_y}. \tag{9}$$

The problem has a load intensity of $L_x = 2$ in the horizontal direction and a load intensity of $L_y = 1$ in the vertical direction. These load intensities are measured in load per unit area where each horizontal element is of unit size. In the horizontal beam where the total cross-sectional area is 3 units, so the horizontal applied load is $F_x = 6$, and in the vertical tie the vertical applied load is $F_y = 1$. Therefore the required cross-sectional area of the vertical tie for a FSD can be obtained as

$$\frac{6}{3} = \frac{1}{A_V} \Rightarrow A_V = \frac{1}{2}. \tag{10}$$

The required element size for the vertical tie is $1/2$ of the original element size. It can therefore be deduced that the vertical tie is eliminated in the first iteration because the vertical tie has a mesh which is too coarse for ESO.

We note that the height of the horizontal beam in Figure 2 is of 1 unit. Thus, to obtain a FSD with a similar height and therefore volume, the necessary refinement to the mesh is determined by substituting $A_x = 1$ into Eq. (9),

$$\frac{6}{1} = \frac{1}{A_V} \Rightarrow A_V = \frac{1}{6}, \tag{11}$$

indicating that the element size needs to be reduced by at least $1/6$ of the original size. We therefore refine the mesh as shown in Figure 4.

B. Application of ESO to the refined mesh

We apply ESO without filtering to the tie beam of Figure 4 with $n = 3600$ plane stress elements and employ von Mises stress as the sensitivity to obtain a FSD. This application of ESO results in the solution of Figure 5, with a volume of $V(\mathbf{x}) = 39$ and a total compliance of $C(\mathbf{x}) = 1030$. We note that the vertical tie remains in the solution.

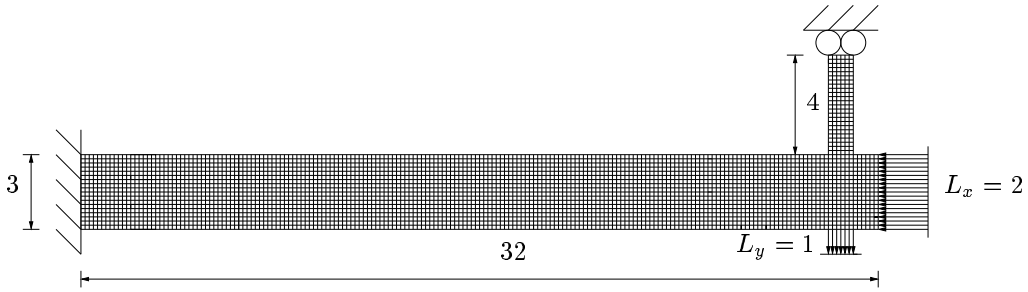

Figure 4. Test problem with a refined mesh

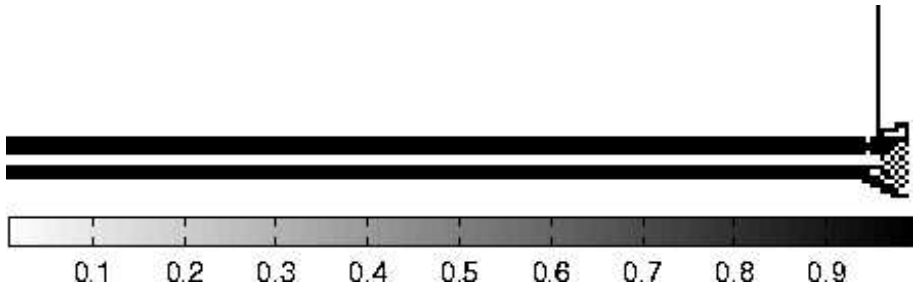

Figure 5. Optimum solution by stress based ESO on a refined mesh, showing a chequerboard pattern to the right of the vertical tie

The solution of Figure 5 is chosen by determining the minimum value of $S(\mathbf{x})$. Figure 6 shows the value of the objective function $S(\mathbf{x})$ with iteration number. The topology of the solution in Figure 5, found after 1091 iterations, is at '*d*' in Figure 6.

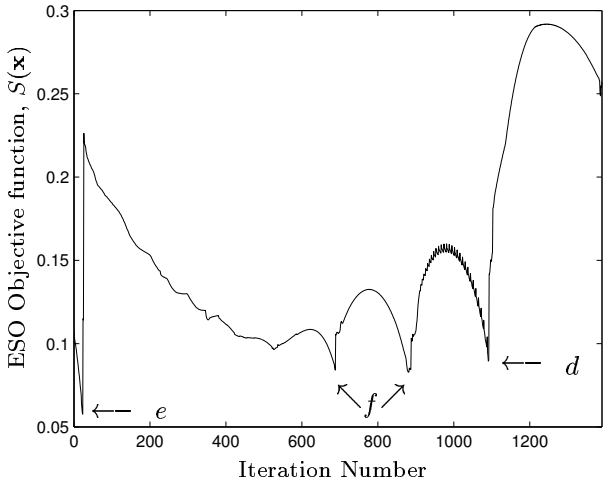

Figure 6. Trajectory of the ESO objective function, $S(\mathbf{x})$, for the refined mesh

Figure 6 reveals however, that there are three other minima of $S(\mathbf{x})$ whereby the lowest is observed after 23 iterations with a compliance of $C(\mathbf{x}) = 392$, highlighted as 'e'. This alternative solution has a volume reduction of only 1% and is illustrated in Figure 7. The other solutions at 'f' are similar to the solution at 'd' except with less of a chequerboard pattern at the beam-tie intersection and with only one solid horizontal beam.

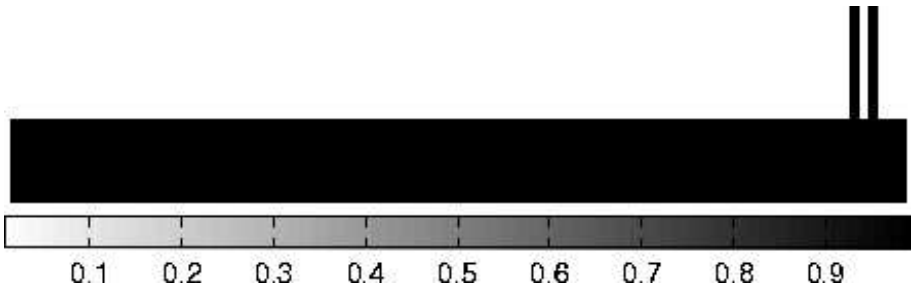

Figure 7. Alternative solution by stress based ESO on a refined mesh

The solution of Figure 5 shows some chequerboard pattern formation near the beam-tie intersection. We therefore apply the filtering technique of §II:C with $r_{min} = 1.5$. This obtains the solution of Figure 8 at $V(\mathbf{x}) = 38$ and a total compliance of $C(\mathbf{x}) = 1080$. This solution has had a majority of the chequerboard patterns removed, and a grillage-like structure is formed at the beam-tie intersection. An examination of the solution of Figure 8 against the intuitive optimum of Figure 2 finds that Figure 8 has a comparable volume and compliance.

Figure 9 shows the trajectory of the ESO objective function $S(\mathbf{x})$ and the solution of Figure 8 is marked 'g'. The minimum of $S(\mathbf{x})$ is again observed at 'h', which is of a similar topology to Figure 7 as shown in Figure 10. There is another optimum at 'l' which is similar to the solution of Figure 8 but has a narrower main beam cross-section.

The two tie configuration solutions as in Figure 10 is favoured by ESO because there exists a local stress concentration at the re-entrant corners. This increases the elemental stresses along the boundary hence favouring the internal elements for removal. This may be considered as a shortcoming of ESO as material cannot be added and therefore the solution is dependent on the initial design. The severe strategy of the complete removal in ESO exacerbates the numerical issues at the sharp corners.

We have demonstrated that the ability of stress based ESO to find a solution for the test problem is dependant on the size of the mesh. If the mesh is of an appropriate size then ESO finds the optimum

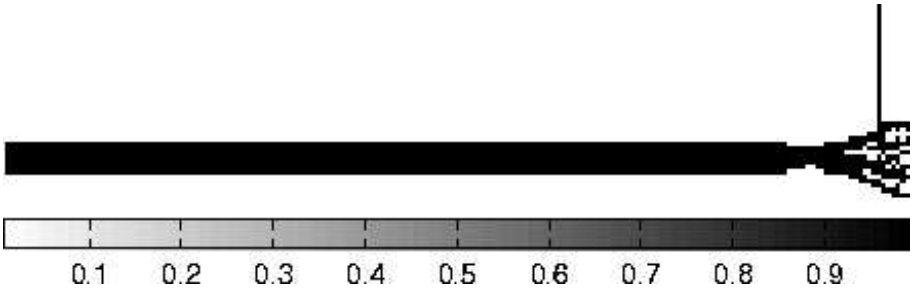

Figure 8. Optimum solution by ESO on a refined mesh using a filter

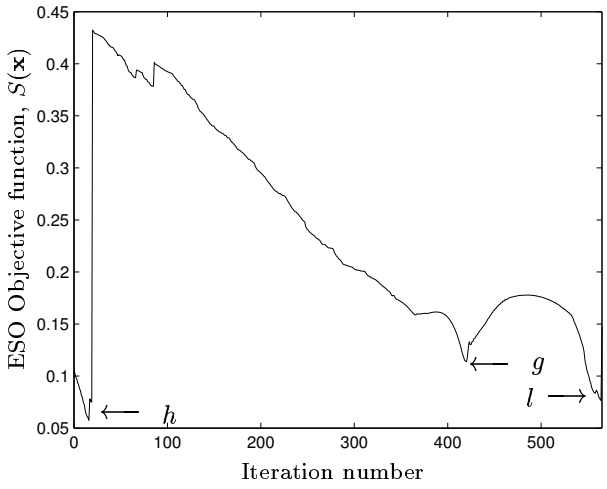

Figure 9. ESO objective function, $S(\mathbf{x})$, for the refined mesh with filtering

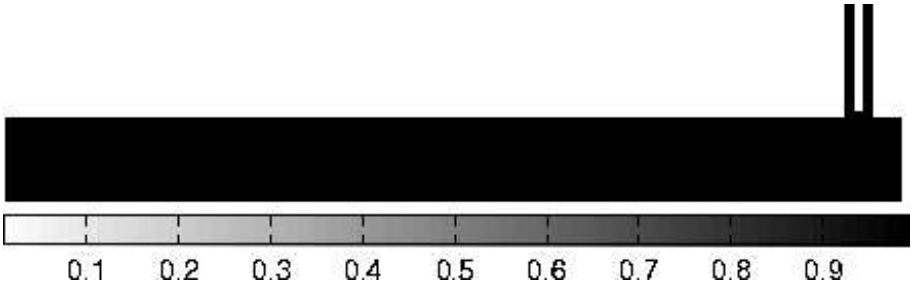

Figure 10. Alternative solution found by stress based ESO on a refined mesh using a filter

configuration.

The optimal solutions found within this section have shown that $S(\mathbf{x})$ defined in Eq. (6) works well as an objective function for ESO. Also filtering gives ESO smoother results.

V. An application of SIMP to the test problem

As a comparison to ESO, we now apply SIMP to the same problem with and without a chequerboard filter. A discrete tie beam solution is only found on one occasion.

A. Minimisation of non-penalised compliance $C(\mathbf{x})$ using the original coarse mesh

We begin this investigation by applying the initial problem of minimum compliance $C(\mathbf{x})$ in Eq. (1) which has no penalisation, to the test problem with the coarse mesh. The converged solution with the volume constraint of $V(\mathbf{x}) \leq 40$ is illustrated in Figure 11 which shows the resulting minimum compliance material distribution plot. The compliance has then been reduced from the initial $C(\mathbf{x}) = 968$ to $C(\mathbf{x}) = 958$ and the optimisation history is given in Figure 12.

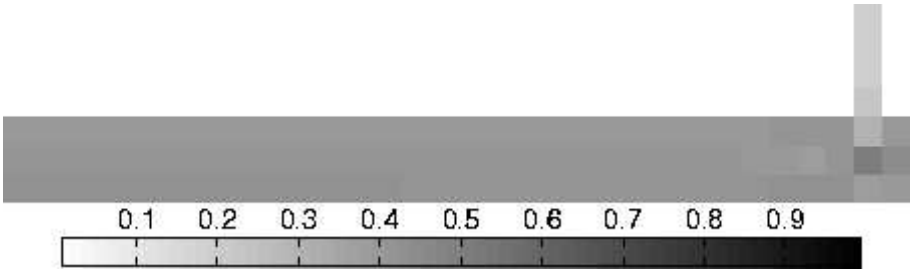

Figure 11. Optimal density distribution $x(\boldsymbol{\xi})$ for SIMP with no penalisation or filter

The solution of Figure 11 has a vertical tie density of $x \approx 0.2$ which is half that of the main beam. This density is greater than the equivalent cross-sectional area of the vertical tie of the ESO results in §IV:B and it can therefore be said that that the loads are carried axially in both solutions. The minimum compliance solution of Figure 11 has reduced overall total compliance but is not discrete.

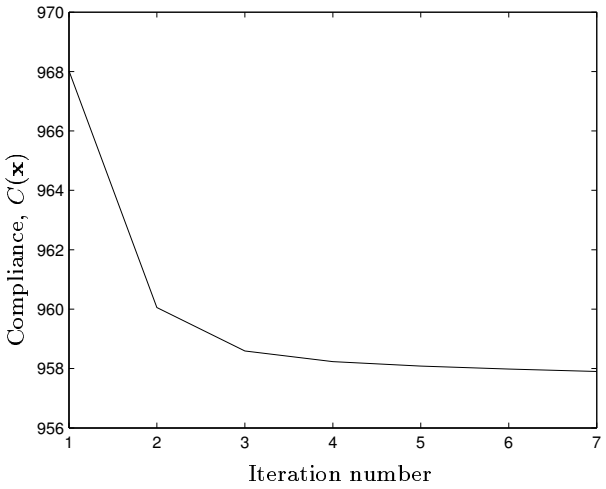

Figure 12. Compliance variation for the solution convergence of the minimum compliance objective applied to the original test problem

B. SIMP optimisation using the original coarse mesh

In order to obtain the minimum compliance discrete solution, we apply the penalisation power $p = 4$ based on $E = 1$ and $\nu = 0$,[15] which gives the solution of Figure 13 at a volume of $V(\mathbf{x}) = 40$.

It is noted that SIMP minimises penalised compliance $C_p(\mathbf{x})$ of Eq. (5) which is plotted with the total compliance against iteration in Figure 12. This plot shows that SIMP minimises monotonically to a minimum penalised compliance solution of $C_p(\mathbf{x}) = 2387$. However, the actual compliance increases from $C(\mathbf{x}) = 968$ to $C(\mathbf{x}) = 1220$. Thus penalised compliance is not equivalent to the total compliance solution. This difference is because the penalisation of the elemental density results in artificially increased displacement and therefore compliance.

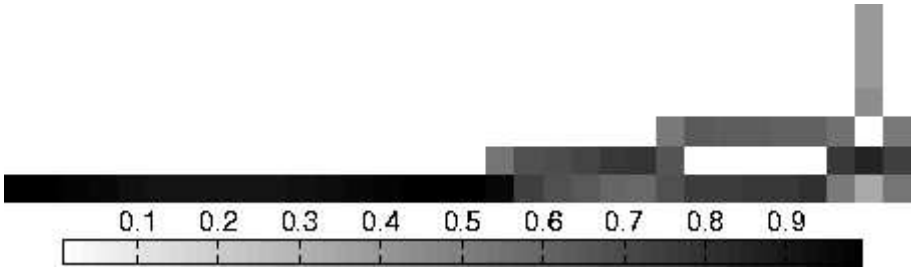

Figure 13. Optimal density distribution for SIMP optimisation without the use of a filter, showing chequerboard-like patterns

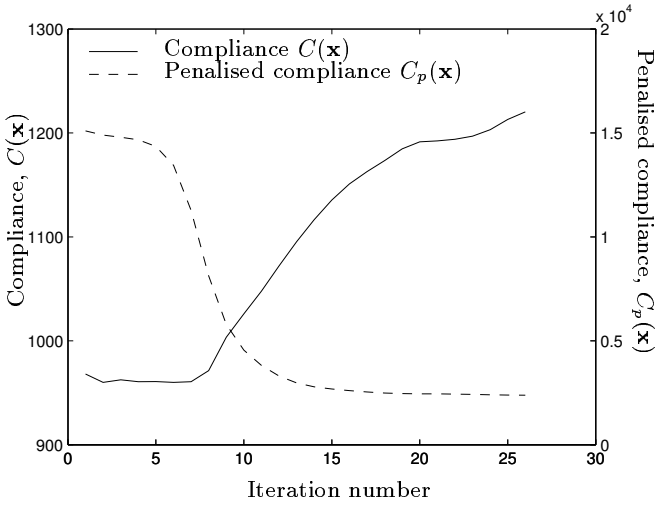

Figure 14. Compliance and penalised compliance variation respectively for the solution convergence of SIMP applied to the original test problem

A chequerboard-like pattern has formed around the beam-tie intersection area of Figure 13. Therefore we apply the filter with $r_{min} = 1.05$ and obtain the optimum solution in Figure 15.

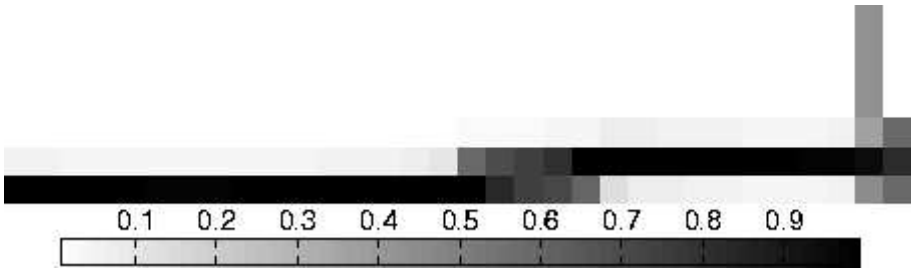

Figure 15. Optimal density distribution for SIMP optimisation using a filter

The filtered solution still has some grey regions but the filter successfully removes the chequerboard-like pattern. However, the optimisation history of compliance and penalised compliance in Figure 16 exhibit similar paths to the unfiltered optimisation of Figure 14. The penalised compliance $C_p(\mathbf{x})$ converges to the minimum solution but the actual total compliance $C(\mathbf{x})$ is still not minimised. Therefore, filtering has not affected the overall convergence of SIMP optimisation.

The total compliance for the topology in Figure 15 is $C(\mathbf{x}) = 1147$, which is a 6% lower than that of the unfiltered equivalent solution of Figure 13. Therefore, using a filter has produced a small reduction

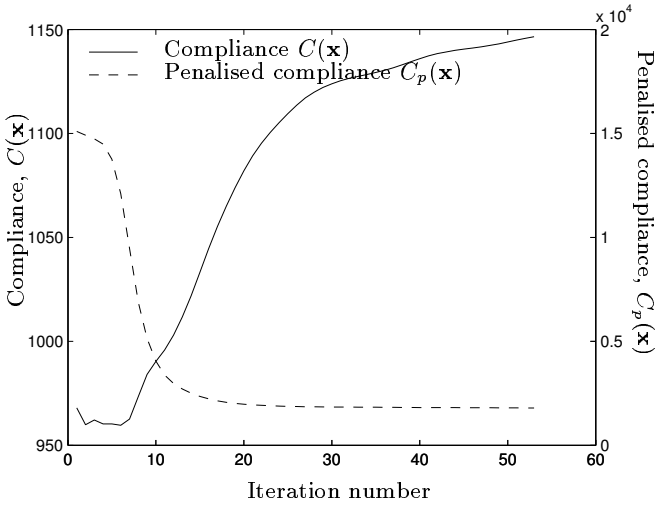

Figure 16. Compliance and penalised compliance variation for the solution convergence of filtered SIMP applied to the original test problem

in actual compliance and a smoother solution. However, it is still 18% higher than the compliance value of the initial design and 3% higher than the intuitive solution of Figure 2.

Returning to the penalised compliance values of the SIMP solutions, Figure 13 (without filtering) has $C_p(\mathbf{x}) = 2387$, and Figure 15 (with filtering) has $C_p(\mathbf{x}) = 1795$. Noting that the intuitive optimum of Figure 2 has a penalised compliance of $C_p(\mathbf{x}) = 1110$, it thus appears that the SIMP approach fails to find that optimum.

C. Examination of the performance of SIMP on the test problem

To understand why SIMP does not produce the discrete tie beam solution of Figure 2, we examine the test problem further. We consider the penalised and total compliance for the intuitive optimum and the initial configuration. When the initial configuration of Figure 1 has a constant density distribution of $x = 0.4$, the total compliance is $C(\mathbf{x}) = 968$ and the penalised compliance is $C_p(\mathbf{x}) = 15099$. The continuous solution presented in Figure 11 has a total compliance of $C(\mathbf{x}) = 958$, successfully found by the minimisation of compliance without penalisation.

In the discrete solution space however, the optimum solution at $V(\mathbf{x}) = 40$ has a total compliance of $C(\mathbf{x}) = C_p(\mathbf{x}) = 1110$, Figure 2. This is greater than the compliance of the initial design, $C(\mathbf{x}) = 968$. Therefore the discrete solution space for the minimisation of the compliance, Eq. (1) is not convex and the discrete optimum of Figure 2 cannot be obtained.

We note however, that the penalised compliance of the initial design at $V(\mathbf{x}) = 40$ is 15099 which is higher than that of the discrete solution, Figure 2. Thus it appears that the objective function of Eq. (5) may still be convex.

D. Rectangular initial design domain

We redefine the test problem by changing the initial design such that the solution space may be convex. We apply SIMP to a rectangular initial design domain of a constant density distribution, Figure 17. Again, the volume constraint of $V(\mathbf{x}) = 40$ is specified. Applying the same loading and boundary conditions, the initial rectangular design has a total compliance of $C(\mathbf{x}) = 1515$ which is higher than the intuitive optimum of Figure 2 and thus appears to have a convex solution space.

With $p = 4$ and no chequerboard filter, indeed, the intuitive discrete solution of Figure 2 is obtained as shown in Figure 18.

Figure 19 displays the optimisation history for both penalised compliance and actual compliance. It shows that, whilst the predicted solution is produced, the compliance function is not convex. Therefore,

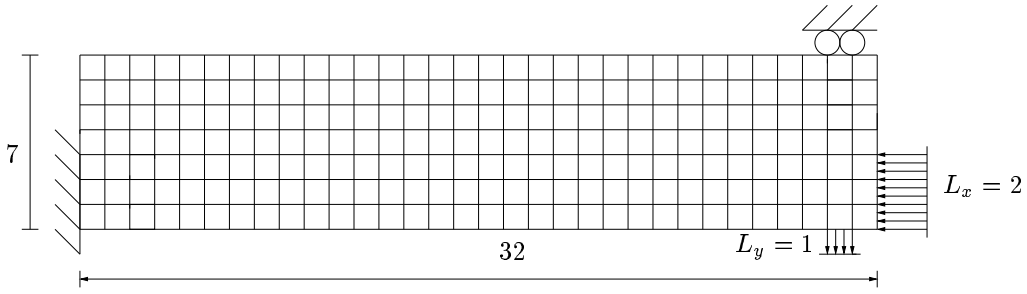

Figure 17. Rectangular initial mesh encompassing original mesh

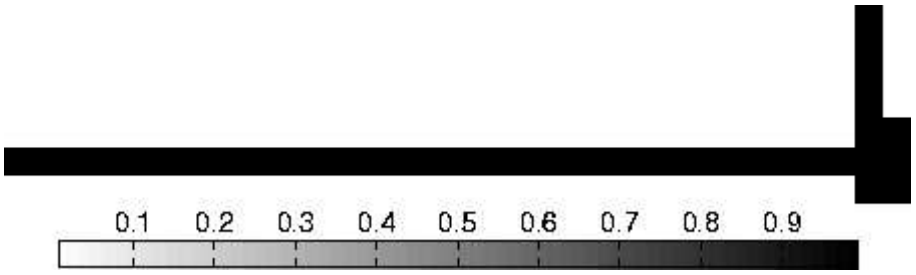

Figure 18. Optimal density distribution for SIMP optimisation without filtering using a rectangular design domain

there exists a solution with lower compliance than the resulting tie beam solution. However, this lower compliance solution contains intermediate density material which has a higher compliance when penalised leading to the tie beam solution.

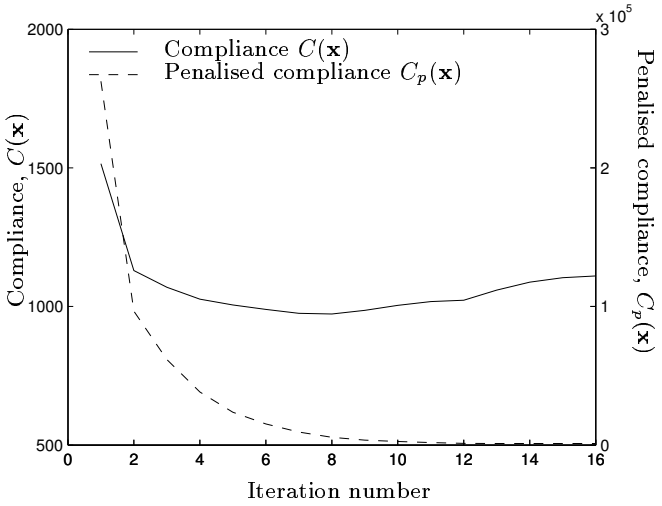

Figure 19. Compliance and penalised compliance optimisation history for SIMP using a rectangular design domain

When SIMP is applied to Figure 17 with a filter of $r_{min} = 1.05$ however, the resulting topology reverts to the similar solution of that obtained from the original design domain (Figure 15) and has a similar total compliance of $C(\mathbf{x}) = 1150$, as shown in Figure 20. This indicates that the filter destabilises and prevents SIMP from finding the discrete tie beam solution of Figure 18.

Figure 21 plots the total and penalised compliance for the filtered solution of Figure 20. In a similar manner to the results found in §V:B, filtering in SIMP does not have a significant influence on the

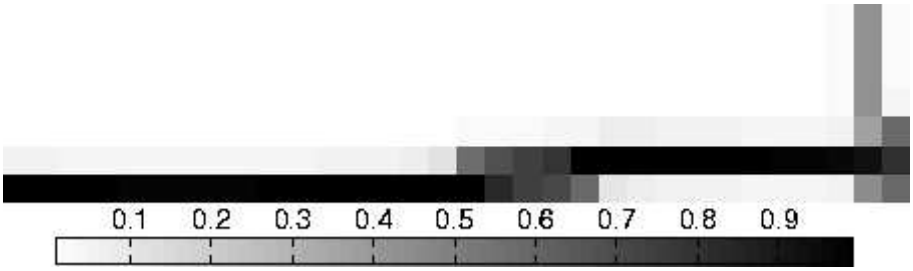

Figure 20. Optimal density distribution for SIMP optimisation with filtering using a rectangular mesh

compliance convergence path.

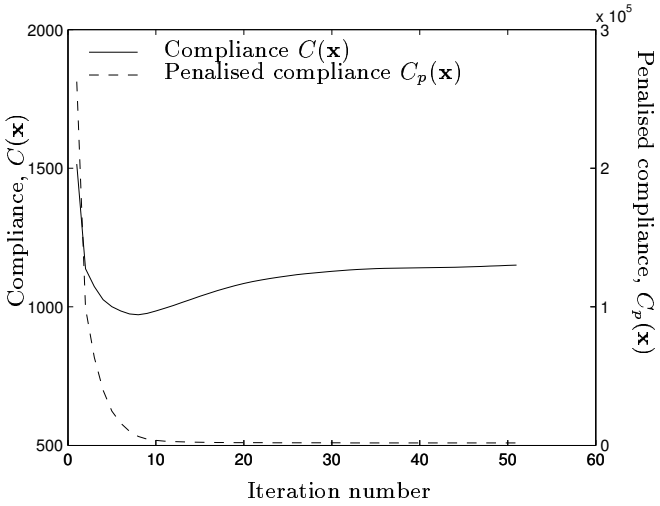

Figure 21. Optimisation history of compliance and penalised compliance for filtered SIMP using a rectangular design domain

VI. Conclusions

Topology optimisation methods of ESO and SIMP are investigated using the tie beam test problem, introduced in Ref. 8. A comprehensive summary of the results is given in Table 1. The results show that both ESO and SIMP are unable to obtain an intuitive optimum also presented in Ref. 8. The reason for this failure in both cases relates to the objective functions of the optimisation methods. However, these reasons are different for ESO and SIMP.

In the past, ESO suffered from having neither a clear definition of the objective function nor an optimisation problem formulation. We propose an appropriate ESO formulation based on the FSD concept, and this is used throughout this investigation to obtain solutions. Applying the FSD criterion to the test problem, a simple analysis indicates that the mesh of the test problem is too coarse for a FSD. It is further demonstrated that an appropriate mesh refinement enables ESO to find a tie beam solution, which compares favourably with the intuitive solution.

It is found that SIMP is unable to find the optimum solution from the original initial design domain for the test problem, but given a rectangular constant density initial design domain, SIMP successfully finds a discrete optimum solution. However, the application of chequerboard filtering appears to have the effect of destabilising the optimisation scheme of SIMP.

This investigation demonstrates that there exists a class of problems which is particularly sensitive to the common numerical treatments of topology optimisation, and special care is required in selecting

Table 1. A summary of all SIMP and ESO solutions

Optimisation method and parameter	Solution		$C(\mathbf{x})$	$V(\mathbf{x})$
Intuitive solution[8]	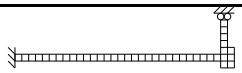	(Figure 2)	1110	40
ESO solution, no filter	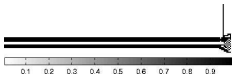	(Figure 5)	1091	39
Alternative ESO solution, no filter	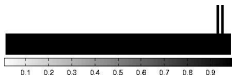	(Figure 7)	392	99
ESO solution, with filter	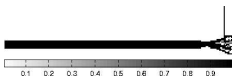	(Figure 8)	1080	38
Alternative ESO solution, with filter	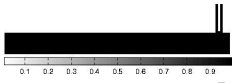	(Figure 10)	392	99
Min. $C(\mathbf{x})$, p=1, no filter		(Figure 11)	958	40
Min. $C_p(\mathbf{x})$, p=4, no filter	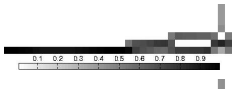	(Figure 13)	1220	40
Min. $C_p(\mathbf{x})$, p=4, with filter	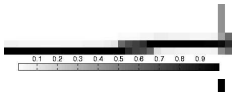	(Figure 15)	1147	40
Min. $C_p(\mathbf{x})$, p=4, rectangular Ω, no filter	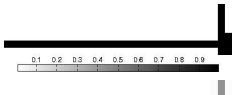	(Figure 18)	1110	40
Min. $C_p(\mathbf{x})$, p=4, rectangular Ω, with filter	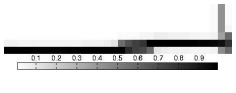	(Figure 20)	1150	40

the mesh density and initial design. In addition, penalisation and filtering techniques can have a destabilising effect on the convergence properties of optimisation schemes. An investigations is underway to understand these effects further.

Acknowledgments

The authors would like to thank Dr Lars Krog, Airbus UK, and Prof Giles Hunt, University of Bath, for their useful advice and discussion. The authors would also like to acknowledge the support of UK Engineering and Physical Sciences Research Council (GR\ S68477) for this research.

References

[1]Sigmund, O. and Petersson, J., "Numerical Instabilities in Topology Optimization: A Survey on Procedures Dealing with Checkerboards, Mesh-dependencies and Local Minima," *Struct. Optim*, Vol. 16, 1998, pp. 68–75.

[2]Bendsøe, M. P., "Optimal Shape Design as a Material Distribution Problem," *Struct. Optim.*, Vol. 1, 1989, pp. 193–202.

[3]Rozvany, G. I. N., Zhou, M., and Birker, T., "Generalized Shape Optimisation Without Homogenisation," *Struct. Optim*, Vol. 4, 1992, pp. 250–254.

[4]Bendsøe, M. P. and Sigmund, O., *Topology Optimization: Theory, Methods and Applications*, Springer, Berlin Heidelberg New York, 2003.

[5]Xie, Y. M. and Steven, G. P., "A Simple Evolutionary Procedure for Structural Optimisation," *Computer and Structures*, Vol. 49, 1993, pp. 885–896.

[6]Xie, Y. M. and Steven, G. P., *Evolutionary Structural Optimization*, Springer, Berlin Heidelberg New York, 1997.

[7]Querin, O. M., *Structural Optimisation: Stress Based Formulation and Implementation*, Ph.D. thesis, University of Sydney, 1997.

[8]Zhou, M. and Rozvany, G. I. N., "On the Validity of ESO Type Methods in Topology Optimization," *Struct Multidisc*

Optim, Vol. 21, 2001, pp. 80–83.

[9]Sigmund, O., "A 99 Line Topology Optimization Code Written in Matlab," *Struc Multidisc Optim*, Vol. 21, 2001, pp. 120–127.

[10]Svanberg, K., "The Method of Moving Asymptotes-A New Method for Structural Optimization," *Int J Num Meth Eng*, Vol. 24, 1987, pp. 359–373.

[11]"MATLAB 7.0," The Math Works, Inc., Natick, Massachusetts, 2004.

[12]Kim, H., Querin, O. M., Steven, G. P., and Xie, Y. M., "A Method for Varying the Number of Cavities in an Optimized Topology Using Evolutionary Structural Optimization," *Struct. Multidisc. Optim*, Vol. 19, 2000, pp. 140–147.

[13]Jog, C. S. and Haber, R. B., "Stability of Finite Element Models for Distributed-Parameter Optimization and Topology Design," *Comput Methods Appl Mech Engrg*, Vol. 130, 1996, pp. 203–226.

[14]Sigmund, O., *Design of Material Structures Using Topology Optimization*, Ph.D. thesis, Technical University of Denmark, 1994.

[15]Bendsøe, M. P. and Sigmund, O., "Material Interpolation Schemes in Topology Optimization Schemes," *Arch Appl Mech*, Vol. 69, 1999, pp. 635–654.